

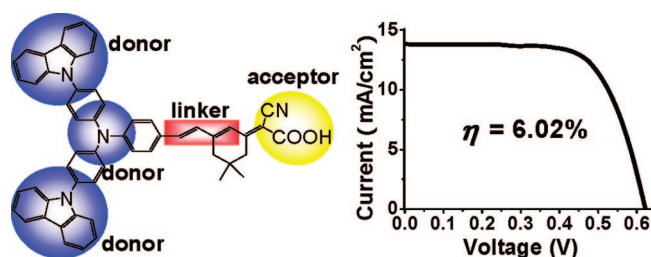
Starburst Triarylamine Based Dyes for Efficient Dye-Sensitized Solar Cells

Zhijun Ning,[†] Qiong Zhang,^{†,‡} Wenjun Wu,[†] Hongcui Pei,[†] Bo Liu,[†] and He Tian^{*,†}

Key Lab for Advanced Materials and Institute of Fine Chemicals, East China University of Science and Technology, 130 Meilong Road, Shanghai, 200237, People's Republic of China, and Theoretical Chemistry, School of Biotechnology, Royal Institute of Technology, S-10691 Stockholm, Sweden

tianhe@ecust.edu.cn

Received January 22, 2008



We report here on the synthesis and photophysical/electrochemical properties of a series of novel starburst triarylamine-based organic dyes (S1, S2, S3, and S4) as well as their application in dye-sensitized nanocrystalline TiO₂ solar cells (DSSCs). For the four designed dyes, the starburst triarylamine group and the cyanoacetic acid take the role of electron donor and electron acceptor, respectively. It was found that the introduction of starburst triarylamine group to form the D-D- π -A configuration brought about superior performance over the simple D- π -A configuration, in terms of bathochromically extended absorption spectra, enhanced molar extinction coefficients and better thermo-stability. Moreover, the HOMO and LUMO energy levels tuning can be conveniently accomplished by alternating the donor moiety, which was confirmed by electrochemical measurements and theoretical calculations. The DSSCs based on the dye S4 showed the best photovoltaic performance: a maximum monochromatic incident photon-to-current conversion efficiency (IPCE) of 85%, a short-circuit photocurrent density (J_{sc}) of 13.8 mA cm⁻², an open-circuit photovoltage (V_{oc}) of 0.63 V, and a fill factor (ff) of 0.69, corresponding to an overall conversion efficiency of 6.02% under 100 mW cm⁻² irradiation. This work suggests that the dyes based on starburst triphenylamine donor are promising candidates for improvement of the performance of the DSSCs.

1. Introduction

Dye-sensitized solar cells (DSSCs) have attracted intense interest for their high performance in converting solar energy to electricity at low cost. The Ru complexes photosensitizers such as the black dye show record solar energy-to-electricity conversion efficiency of 11%.^{1,2} Recently, organic DSSCs have received more and more attention for their variety, high molar extinction coefficients, and simple preparation process of low cost in comparison to Ru complexes. Metal-free dyes such as

perylene dyes,³ cyanine dyes,⁴ merocyanine dyes,⁵ coumarin dyes,⁶ hemicyanine dyes,⁷ and indoline dyes⁸ have been investigated as sensitizers for DSSC.

* To whom correspondence should be addressed. Tel: +86-21-64252756. Fax: +86-21-64252288.

[†] East China University of Science and Technology.

[‡] Royal Institute of Technology.

(1) (a) O'Regan, B.; Grätzel, M. *Nature* **1991**, 353, 737. (b) Robertson, N. *Angew. Chem., Int. Ed.* **2006**, 45, 2338.

(2) (a) Nazeeruddin, M. K.; Zakeeruddin, S. M.; Humphry-Baker, R.; Jirousek, M.; Liska, P.; Vlachopoulos, N.; Shklover, V.; Fisher, C.-H.; Grätzel, M. *Inorg. Chem.* **1999**, 38, 6298. (b) Nazeeruddin, M. K.; Péchy, P.; Renouard, T.; Zakeeruddin, S. M.; Humphry-Baker, R.; Comte, P.; Liska, P.; Cevey, L.; Costa, E.; Shklover, V.; Spiccia, L.; Deacon, G. B.; Bignozzi, C. A.; Grätzel, M. *J. Am. Chem. Soc.* **2001**, 123, 1613.

(3) (a) Ferrere, S.; Zaban, A.; Gregg, B. A. *J. Phys. Chem. B* **1997**, 101, 4490. (b) Ferrere, S.; Gregg, B. A. *New J. Chem.* **2002**, 26, 1155. (c) Tian, H.; Liu, P.-H.; Zhu, W.; Gao, E.-Q.; Wu, D.-J.; Cai, S.-M. *J. Mater. Chem.* **2000**, 10, 2708. (d) Tian, H.; Liu, P.-H.; Meng, F.-S.; Gao, E.-Q.; Cai, S.-M. *Synth. Met.* **2001**, 121, 1557.

(4) (a) Yao, Q.-H.; Meng, F.-S.; Li, F.-Y.; Tian, H.; Huang, C.-H. *J. Mater. Chem.* **2003**, 13, 1048. (b) Sayama, K.; Hara, K.; Ohga, Y.; Shinpou, A.; Suga, S.; Arakawa, H. *New J. Chem.* **2001**, 25, 200. (c) Ehret, A.; Stuhl, L.; Spitzler, M. T. *J. Phys. Chem. B* **2001**, 105, 9960.

Most organic sensitizers are constituted by donor, linker, and acceptor moieties and usually have the rod-like configuration. Generally, organic dyes used for efficient solar cells are required to possess broad and intense spectral absorption in the visible light region. One strategy toward this end is to introduce more π -conjugation segments between the donor and acceptor, thereby forming a D- π - π -A structure.⁹ However, one aftermath with this approach is that the rod-like molecules are prolonged, which may facilitate the recombination of electrons to the triiodide and aggravate aggregation between molecules.¹⁰ The close π - π aggregation can not only lead to self-quenching and reduction of electron injection into TiO₂ but also to the instability of the organic dyes due to the formation of excited triplet states and unstable radicals under light irradiation.¹¹ Recently, the notion of incorporating a nonplanar triphenylamine or bis-dimethylfluorenylamino moiety into the organic framework was proposed. In this way, the conversion efficiency has reached record 9.1% and the performance of the cells can be retained over 1200 h without obvious decline.¹² We expect that a further improvement could be made by introducing starburst triarylamino group into the molecule to form the D-D- π -A structure. On one hand, the absorption region can be extended and the molar extinction coefficient can be enhanced comparing with the D- π -A structure. On the other hand, they benefit from lower tendency to aggregate and better thermo-stability.

Furthermore, the starburst triarylamino and carbazole molecules have aroused great interest for their excellent hole-transport capability, and they have become classic hole-transporting materials.¹³ Recently, it has been found that by incorporating electron donor triarylamino group into the dye molecules, the physical separation of the dye cation from the electrode surface will be increased, which fascinates to achieve

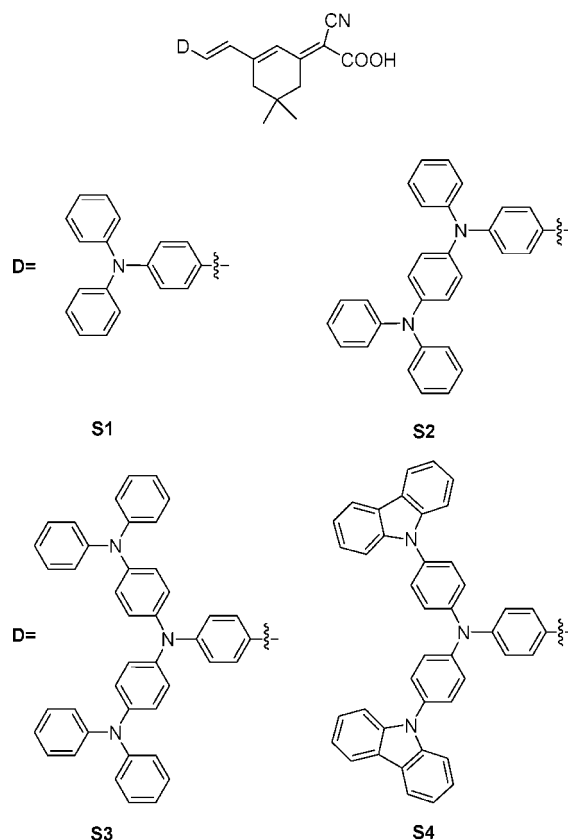


FIGURE 1. Molecular structures of dyes in this study.

high rates of charge separation and collection compared to interfacial charge-recombination processes.¹⁴ It is natural to assume that this effect will be further reinforced by incorporating starburst dendronized triarylamino moiety into the molecule.

Based on the above consideration, we have designed and synthesized the novel unsymmetrical organic sensitizers S1, S2, S3, and S4 (see Figure 1) that consist of the starburst triarylamino moiety acting as electron donor and cyanoacrylic acid moiety acting as acceptor, the two functions being connected by conducting isophorone unit.

2. Results and Discussion

The synthetic route of all dyes is depicted in Scheme 1. The bridging isophorone units are employed to provide conjugation between the donor and the anchoring groups as well as to increase the molar extinction coefficients of the dyes. The aldehyde triarylamino were synthesized according to the previously reported method.^{13c} The Knoevenagel condensation of the respective aldehyde triarylamino intermediate and ethyl 2-cyano-2-(3,5,5-trimethylcyclohex-2-enylidene)acetate led to the ester precursors, the hydrolyses of which directly yielded the final products.

Absorption spectra of all compounds in dilute solution of CHCl₃ are shown in Figure 2. All the compounds exhibit two major prominent bands, appearing at 300–330 and at 480–530 nm, respectively. The former is ascribed to a localized aromatic π - π^* transition and the later is of charge-transfer character. The extinction coefficients of the former absorption band of S2, S3,

(5) (a) Khazraji, A. C.; Hotchandani, S.; Das, S.; Kamat, P. V. *J. Phys. Chem. B* **1999**, *103*, 4693. (b) Sayama, K.; Hara, K.; Mori, N.; Satsuki, M.; Suga, S.; Tsukagoshi, S.; Abe, Y.; Sugihara, H.; Arakawa, H. *Chem. Commun.* **2000**, 1173.

(6) (a) Hara, K.; Sayama, K.; Ohga, Y.; Shinpo, A.; Suga, S.; Arakawa, H. *Chem. Commun.* **2001**, 569. (b) Wang, Z.-S.; Cui, Y.; Hara, K.; Dan-oh, Y.; Kasada, C.; Shinpo, A. *Adv. Mater.* **2007**, *19*, 1138. (c) Hara, K.; Kurashige, M.; Danoh, Y.; Kasada, C.; Shinpo, A.; Suga, S.; Sayama, K.; Arakawa, H. *New J. Chem.* **2003**, *27*, 783.

(7) (a) Stathatos, E.; Lianos, P.; Laschewsky, A.; Ouari, O.; Van Cleuvenbergen, P. *Chem. Mater.* **2001**, *13*, 3888. (b) Wang, Z. S.; Li, F. Y.; Huang, C. H. *Chem. Commun.* **2000**, 2063.

(8) (a) Horiuchi, T.; Miura, H.; Uchida, S. *Chem. Commun.* **2003**, 3036. (b) Horiuchi, T.; Miura, H.; Sumioka, K.; Uchida, S. *J. Am. Chem. Soc.* **2004**, *126*, 12218.

(9) (a) Velusamy, M.; Thomas, K. R. J.; Lin, J. T.; Hsu, Y.-C.; Ho, K.-C. *Org. Lett.* **2005**, *7*, 1899. (b) Li, L. S.; Jiang, K. J.; Shao, K. F.; Yang, L. M. *Chem. Commun.* **2006**, 2792. (c) Chen, R.; Yang, X.; Tian, H.; Wang, X.; Hagfeldt, A.; Sun, L. *Chem. Mater.* **2007**, *19*, 4007. (d) Chen, R. K.; Yang, X. C.; Tian, H. N.; Sun, L. C. *J. Photochem. Photobiol. A: Chem.* **2007**, *189*, 295.

(10) Hagberg, D. P.; Marinado, T.; Karlsson, K. M.; Nonomura, K.; Qin, P.; Boschloo, G.; Brinck, T.; Hagfeldt, A.; Sun, L. *J. Org. Chem.* **2007**, *72*, 9550.

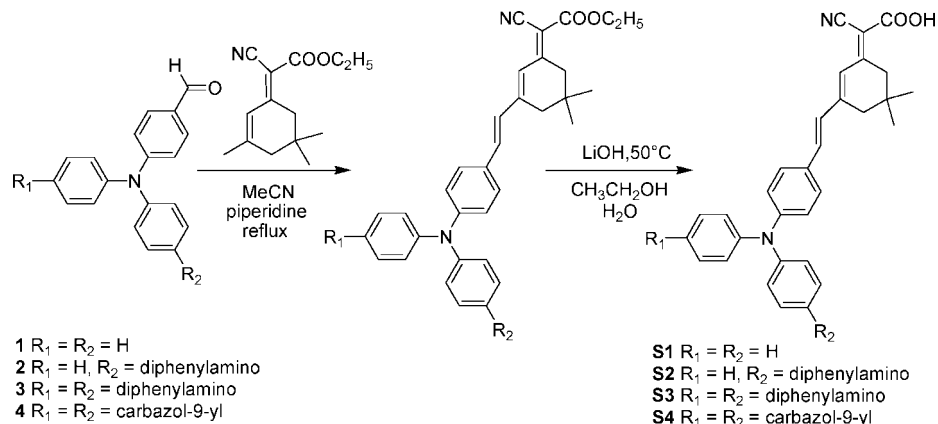
(11) Liu, D.; Fessenden, R. W.; Hug, G. L.; Kamat, P. V. *J. Phys. Chem. B* **1997**, *101*, 2583.

(12) (a) Kim, S. Lee.; J. K.; Kang, S. O.; Ko, J.; Yum, J.-H.; Fantacci, S.; De Angelis, F.; Di Censo, D.; Nazeeruddin, Md. K.; Grätzel, M. *J. Am. Chem. Soc.* **2006**, *128*, 16701. (b) Choi, H.; Baik, C.; Kang, S. O.; Ko, J.; Kang, M.-S.; Nazeeruddin, Md. K.; Grätzel, M. *Angew. Chem., Int. Ed.* **2008**, *47*, 327. (c) Hwang, S.; Lee, J. H.; Park, C.; Lee, H.; Kim, C.; Park, C.; Lee, M.-H.; Lee, W.; Park, J.; Kim, K.; Park, N.-G.; Kim, C. *Chem. Commun.* **2007**, 4887. (d) Thomas, K. R. J.; Lin, J. T.; Hsu, Y. C.; Ho, K. C. *Chem. Commun.* **2005**, 4098. (e) Hagberg, D. P.; Edvinsson, T.; Marinado, T.; Boschloo, G.; Hagfeldt, A.; Sun, L.-C. *Chem. Commun.* **2006**, 2245. (f) Liang, M.; Xu, W.; Cai, F.; Chen, P.; Peng, B.; Chen, J.; Li, Z. *J. Phys. Chem. C* **2007**, *111*, 4465. (g) Tsai, M.-S.; Hsu, Y.-C.; Lin, J. T.; Chen, H.-C.; Hsu, C.-P. *J. Phys. Chem. C* **2007**, *111*, 18785. (h) Thomas, K. R. J.; Hsu, Y.; Lin, J. T.; Lee, K.; Ho, K.; Lai, C.; Cheng, Y.; Chou, P. *Chem. Mater.* **2008**, *20*, 1830.

(13) (a) Shirota, Y. *J. Mater. Chem.* **2000**, *10*, 1. (b) Shirota, Y. *J. Mater. Chem.* **2005**, *15*, 75. (c) Ning, Z. J.; Chen, Z.; Zhang, Q.; Yan, Y. L.; Qian, S. X.; Tian, H.; Cao, Y. *Adv. Funct. Mater.* **2007**, *17*, 3799.

(14) (a) Hirata, N.; Lagref, J.-J.; Palomares, E. J.; Durrant, J. R.; Nazeeruddin, M. K.; Grätzel, M.; Censo, D. *Chem.-Eur. J.* **2004**, *10*, 595. (b) Karthikeyan, C. S.; Wietasch, H.; Thelakkat, M. *Adv. Mater.* **2007**, *19*, 1091.

SCHEME 1. Synthesis of the Chromophores



and S4 are larger than that of S1, which is the result of the increase of the conjugation length. For the π - π^* transitions of conjugated chromophores, extinction coefficients are higher as the enhancement of the conjugation length.^{12e} The larger extinction coefficient of the π - π^* transition band in S3 than in S2 can be attributed to the increase of the number of triarylamine units. This is consistent with the computation result that the oscillation strength of the second absorption band of S3 is higher than S2. However, the charge transfer band has a larger extinction coefficient in S2 than in S3. It has been speculated that it may be caused by the decrease of coplanarity between the electron donor and the electron acceptor in the ground-state as well as in the Franck–Condon excited-state because of the starburst triarylamine structure in S3.^{12h} In progressing from S1, S2, to S3, the absorption spectra (Table 1) show a bathochromic shift of the maximum absorption and an extension to longer wavelength. Moreover, the molar extinction coefficients of S4, S2, and S3 are all higher than S1. It is confirmed that this is an effective way to bathochromically shift the absorption spectrum and enhance the molar extinction coefficients by forming the D-D- π -A structure. The greater maximum absorption coefficients of the organic dyes allow a correspondingly thinner nanocrystalline film so as to avoid the decrease of the film mechanical strength. This also benefits the electrolyte diffusion in the film and reduces the recombination possibility of the light-induced charges during recombination.⁵ The absorption spectra adsorbed on TiO₂ are shown in Figure 3. In comparison with S1, the absorption spectra of S4, S2, and S3 are broader, which is an advantageous spectral property for light harvesting of the solar spectrum. The broad absorption region of all dyes loaded on the TiO₂ film might be caused by the slight aggregation of dyes on the TiO₂ film.^{9d,12f} The

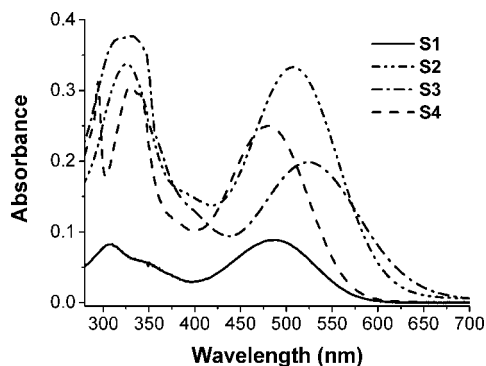


FIGURE 2. Absorption spectra of dyes in CHCl₃ (1×10^{-5} M).

TABLE 1. Photophysical Parameters of the Dyes

dye	$\lambda_{\max}^a/\text{nm}(\epsilon \times 10^{-4}\text{M}^{-1}\text{cm}^{-1})$	$\lambda_{\max}^b/\text{nm}$	$\lambda_{\text{em}}^c/\text{nm}$	amount ^d / 10^{-8} mol cm ⁻²
S1	487 (0.885), 307 (0.823)	481	642	4.6
S2	508 (3.33), 325 (3.37)	487	-	3.8
S3	522 (1.98), 329 (3.78)	479	-	3.2
S4	480 (2.50), 329 (3.05), 293 (3.10)	505	653	3.5

^a Absorption maximum in CHCl₃. ^b Absorption maximum on TiO₂ film. ^c Emission maximum of the dyes in CHCl₃. S1 and S4 are excited at 487 and 480 nm, respectively. ^d Amount of the dyes adsorbed on TiO₂ film.

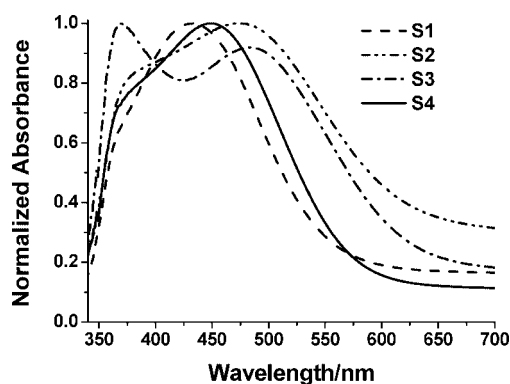


FIGURE 3. Absorption spectra of dyes recorded in the TiO₂ film.

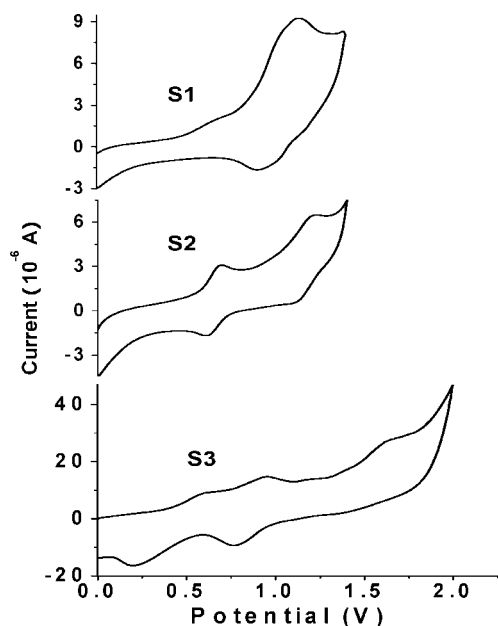
emission spectra also display a slight red-shift upon increased donor moiety (see Table 1).

To evaluate the possibility of electron transfer from the excited dye molecule to the conductive band of TiO₂, cyclic voltammograms were performed in CH₂Cl₂ solution, using 0.1 M tetrabutylammonium hexafluorophosphate as a supporting electrolyte. All the dyes demonstrate reversible redox waves at a moderately high oxidation potential (Figure 4). S2 exhibits two reversible processes in the oxidation scan that correspond to the oxidations of the two triphenylamine units in the donor moiety, whereas S3 displays three reversible oxidation processes in accordance with three triphenylamine units. The examined highest occupied molecular orbital (HOMO) levels and the lowest unoccupied molecular orbital (LUMO) levels are listed in Table 2. The oxidation potential for S3 and S2 are significantly lower than S1. By alternating the donor group independently, we can systematically record the contributions of different groups and attain a HOMO and LUMO energy library.¹⁰ This screening strategy helps us to optimize the TiO₂-dye-hole transporting materials system in terms of balance

TABLE 2. HOMO and LUMO Values for S1, S2, S3, and S4

dye	HOMO ^a (eV)	LUMO ^a (eV)	HOMO ^b (eV)	LUMO ^b (eV)	HOMO ^c (eV)	LUMO ^c (eV)
S1	-5.32	-3.16	-5.12	-2.52	-5.04	-2.57
S2	-4.94	-2.77	-4.85	-2.48	-4.75	-2.55
S3	-4.71	-2.48	-4.72	-2.44	-4.64	-2.53
S4	-5.71	-3.54	-5.18	-2.64	-5.05	-2.61

^a HOMO is derived by a comparison with the ionization potential of ferrocene, scan rate, 100 mV/sec; LUMO is calculated from the oxidation potential and the energy at the crossing section of absorption and emission spectra. ^b Calculated at the B3LYP/6-31G* level in vacuo. ^c Calculated at the B3LYP/6-31G* level in CHCl₃.

FIGURE 4. Oxidative cyclic voltammetry plots measured in CH₂Cl₂.

between photovoltage, driving forces, and spectral response for future preparation of highly efficient dyes by matching suitable donor-linker-acceptor components.¹⁵ The HOMO potential of the dye should be sufficiently positive compared to the electrolyte redox potential for efficient dye regeneration.¹⁶ The small gap between the electrolyte and the oxidation potential of S2 and S3 may affect the effective electron transfer between them. However, considering their excellent hole transporting ability, they should be more promising in the future solid state solar cells.¹⁷ Judging from the LUMO value, the excited-state energy levels for the products are much higher than the bottom of the conduction band of TiO₂ (-4.4 eV), indicating that the electron injection process from the excited dye molecule to TiO₂ conduction band is energetically viable.

To gain insight into the geometrical, electronic, and optical properties of these dyes, we mimicked the optimized geometries of S4, S3 and S1 (Figure S1, Supporting Information) by hybrid density functional theory (B3LYP) with 6-31G* basis set as implemented in the Gaussian 03 program.¹⁸ All dihedral angles between the phenyl planes are listed in Table S1 (see Supporting Information) and they are all noncoplanar with each other. The

angles formed between carbazole and benzene plane in S4 are as large as 55.89°, which can help to inhibit the close π - π aggregation effectively between the starburst structures. The noncoplanar configuration can also reduce contact between molecules and enhance their thermo-stability.¹⁹ The thermal properties of S1 and S4 were examined. The melting point of S1 and S4 were measured to be 175 and 210 °C respectively. The decompose temperature were determined to be 335 and 405 °C for S1 and S4, respectively, when they were decomposed to 95% weight. It is obvious that the thermo-stability of starburst S4 is superior to S1. The better thermo-stability of the sensitizer S4 is critical for the lifetime of the solar cells.¹²

We also mimicked the electronic structure of sensitizers both in vacuo and in CHCl₃ solution, which is the solvent used to record the experimental spectra. It was found that inclusion of solvation effects does not lead to a qualitative change in the electronic structure, even though smaller HOMO–LUMO gaps were calculated as compared to the gas phase. The electron distribution of the HOMO and LUMO of S1, S4, and S3 are shown in Figure 5 (larger pictures of HOMO–LUMO levels are shown in Figure S2, Supporting Information). The HOMO of these compounds is delocalized over the starburst triarylamine moiety, with maximum components arising from the nitrogen lone-pair and the π framework of the surrounding ligands. The LUMO is a π^* orbital delocalized across the 2-cyano-2-(5,5-dimethylcyclohex-2-enylidene) acetic acid group, with sizable components from the cyano- and carboxylic moieties. Distributions of HOMO and LUMO levels are separated in all compounds indicating that the HOMO–LUMO transition can be consider as a charge-transfer transition.²⁰ As expected, the HOMO and LUMO levels increase when increasing the number of electron-donating groups in the molecule, in agreement with the electrochemical results. As is shown in Figure 4, the increase of the triarylamine units in S2 and S3 leads to the increase number of orbital from which two or three electrons can be successively removed, in correspondence with the two or three oxidative processes in the cyclic voltammograms. Calculations also show that the HOMO–LUMO gap ΔE decreases with the increment of the number of electro-donor groups in the molecule, which is in qualitative agreement with experimental absorption spectra and electrochemical results.

(15) Leriche, P.; Frère, P.; Cravino, A.; Alévêque, O.; Roncali, J. *J. Org. Chem.* **2007**, *72*, 8332.

(16) Qin, P.; Yang, X.; Chen, R.; Sun, L. C.; Marinado, T.; Edvinsson, T.; Boschloo, G.; Hagfeldt, A. *J. Phys. Chem. C* **2007**, *111*, 1853.

(17) (a) Johansson, E. M.J.; Karlsson, P. G.; Hedlund, M.; Ryan, D.; Siegbahn, H.; Rensmo, H. *Chem. Mater.* **2007**, *19*, 2071. (b) Roquet, S.; Cravino, A.; Leriche, P.; Aleveque, O.; Frere, P.; Roncali, J. *J. Am. Chem. Soc.* **2006**, *128*, 3459.

(18) Frisch, M. J.; Trucks, G. W.; Schlegel, H. B.; Gill, P. M. W.; Johnson, B. G.; Robb, M. A.; Cheeseman, J. R.; Keith, T.; Petersson, G. A.; Montgomery, J. A.; Raghavachari, K.; Al-Laham, M. A.; Zakrzewski, V. G.; Ortiz, J. V.; Foresman, J. B.; Cioslowski, J.; Stefanov, B. B.; Nanayakkara, A.; Challacombe, M.; Peng, C. Y.; Ayala, P. Y.; Chen, W.; Wong, M. W.; Andres, J. L.; Replogle, E. S.; Gomperts, R.; Martin, R. L.; Fox, D. J.; Binkley, J. S.; Defrees, D. J.; Baker, J.; Stewart, J. P.; Head-Gordon, M.; Gonzalez, C.; Pople, J. A. *Gaussian 03*, revision C.01; Gaussian, Inc.: Pittsburgh, PA, 2004.

(19) Ning, Z. J.; Zhou, Y. C.; Zhang, Q.; Ma, D. G.; Zhang, J. J.; Tian, H. *J. Photochem. Photobiol. A: Chem.* **2007**, *192*, 8.

(20) (a) Coropceanu, V.; Cornil, J.; da Silva Filho, D. A.; Olivier, Y.; Silbey, R.; Brédas, J.-L. *Chem. Rev.* **2007**, *107*, 926. (b) Lemaur, V.; Steel, M.; Beljonne, D.; Brédas, J.-L.; Cornil, J. *J. Am. Chem. Soc.* **2005**, *127*, 6077. (c) Cornil, J.; Beljonne, D.; Calbert, J. P.; Brédas, J. L. *Adv. Mater.* **2001**, *13*, 1053.

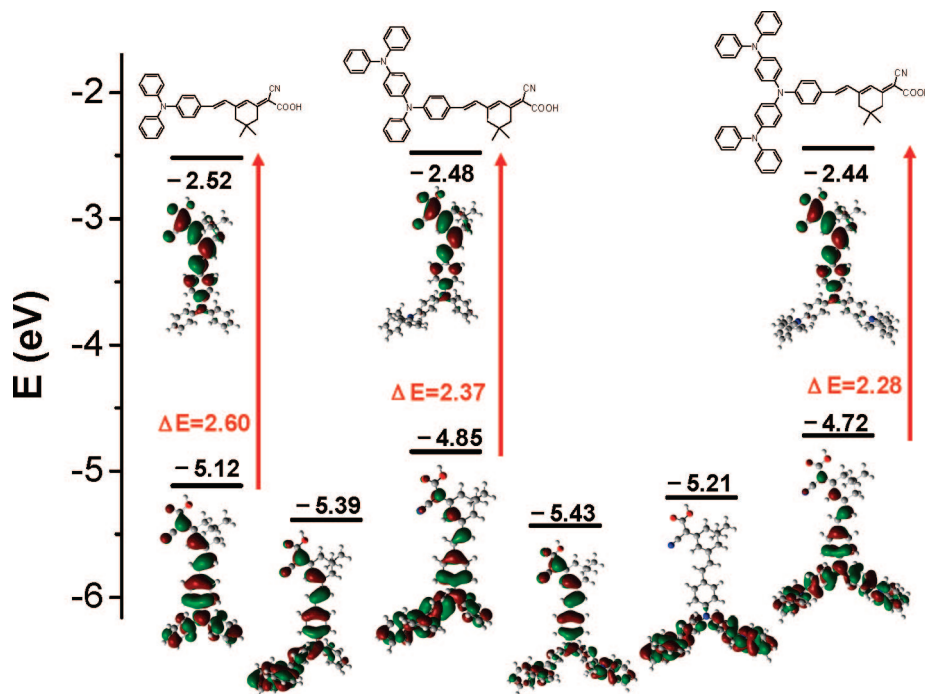


FIGURE 5. Calculated HOMO and LUMO levels for compounds S1, S2, and S3.

TABLE 3. Calculated TDDFT Excitation Energies for the Lowest Transition (eV, nm), Oscillator Strengths (f), Composition in Terms of Molecular Orbital Contributions, and Experimental Absorption Maxima

compounds	state	composition ^a	E (eV, nm)	f	exp. (eV, nm)
S1	S ₁	85% H→L	2.42(513)	1.0404	2.55(487)
	S ₂	75% H1→L	3.30(375)	0.4585	4.04(307)
S2	S ₁	67% H→L	2.14(578)	0.5927	2.44(508)
	S ₂	84% H1→L	2.71(457)	0.6770	3.81(325)
S3	S ₁	67% H→L	2.05(604)	0.6711	2.38(522)
	S ₂	70% H1→L	2.50(496)	0.0314	
	S ₃	64% H2→L	2.81(440)	0.8287	3.77(329)
S4	S ₁	67% H→L	2.30(539)	0.6987	2.58(480)
	S ₂	70% H1→L	2.62(473)	0.0252	
	S ₃	67% H2→L	2.80(442)	0.5765	3.77(329)

^a H = HOMO, L = LUMO, H1 = next highest occupied molecular orbital, or HOMO-1, H2 = HOMO-2.

To gain insight into the excited states giving rise to the optically active absorption bands in the visible region, we performed TDDFT excited states calculations at the B3LYP/6-31G* level in vacuo with the B3LYP/6-31G* optimized ground-state geometries, given the negligible effect of solvation on the electronic structure. The lowest transition of all compounds is listed in Table 3 and corresponds to a charge-transfer excitation from the triarylamine HOMO to the LUMO, localized on 2-cyano-2-(5,5-dimethylcyclohex-2-enylidene) acetic acid acceptor. The absorption wavelength increases with the increase of the donor moiety, which is in qualitative agreement with experimental absorption spectra. For S3, there is a particular charge transfer state compared with S1 and S2. The S₂ transition state has charge shift mainly from the two outer triarylamine moieties to the 2-cyano-acrylic acid, as reflected by their molecular orbital involved in the transition as well as the low oscillator strength due to the long-range charge shift. This means that this extra donor unit may cause a cascading effect in aiding the charge separation.^{12g} We speculate that this is the reason for the slightly larger short-circuit current of S3 than S2 (see below for the result).

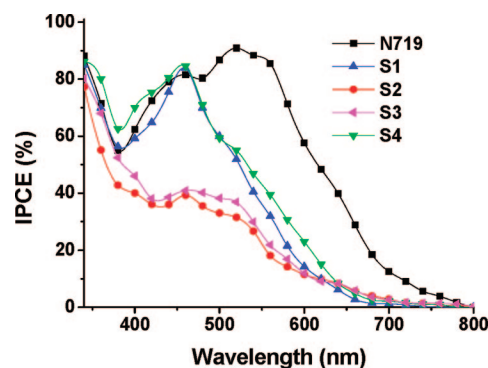


FIGURE 6. Photocurrent action spectra of the TiO₂ electrodes sensitized by dyes.

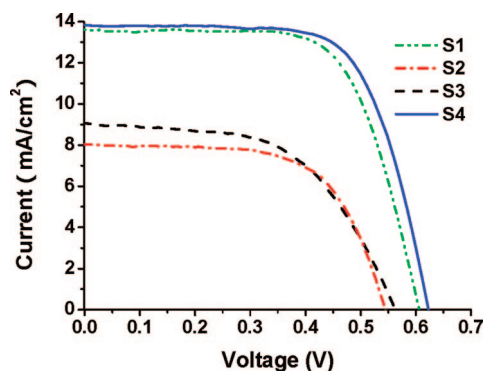
Figure 6 shows the incident monochromatic photon-to-current conversion efficiency (IPCE) obtained with a sandwich cell using 0.5 M 1-methyl-3-propyl imidazolium iodide, 0.1 M LiI, 0.05 M I₂, 0.3 M tert-butylpyridine in a 7/3 (v/v) mixture of acetonitrile and 3-methoxy-propionitrile as redox electrolyte. The IPCE data of S4 sensitizer plotted as a function of excitation wavelength exhibit a strikingly high efficiency of 85%. The IPCE spectra of them are consistent with the absorption spectra on the TiO₂ film. The maximum IPCE values of S2 and S3 are significantly lower than S1 and S4, whereas in the long wavelength region S2 and S3 show a little higher IPCE, which is in accordance with their absorption spectra on the TiO₂ film.

The photoelectrochemical properties of dyes sensitized TiO₂ electrodes under irradiation of Xe lamp (100mW cm⁻²) are listed in Table 4, and the corresponding photocurrent–voltage curves are shown in Figure 7. S4 shows the highest efficiency among the four dyes. The open-circuit photovoltage and overall yield for the four dyes lie in the order S4 > S1 > S3 > S2. The short-circuit current and open-circuit voltage of S2 and S3 are lower than S1 and S4, which can be attributed to the poor injection efficiency of the dyes. This may be the result of the small energy gap between electrolyte and dyes or their unfavor-

TABLE 4. Performance Parameters of Dye-Sensitized Solar Cells^a

dye	J_{sc} (mA/cm ²)	V_{oc} (V)	ff	η (%)
S1	13.6	0.615	0.69	5.77
S2	8.02	0.543	0.64	2.79
S3	9.05	0.567	0.56	2.87
S4	13.8	0.632	0.69	6.02
N719	18.5	0.648	0.65	7.79

^a The listed data are results from the measurement which has the closest values to the average of 10 times measurements.

**FIGURE 7.** Photocurrent–voltage curves of dyes sensitized TiO₂ electrodes.

able absorption pattern on the TiO₂ surface.¹⁰ The slightly larger short-circuit current of S3 than S2 can be tentatively attributed to cascade electron transfer from the starburst triarylamine group to the acceptor moiety. The open-circuit voltage of S4 is higher than S1, for the starburst triarylamine structure might be beneficial for retarding the electron transfer from TiO₂ to the oxidized dye or electrolyte, which would enhance the open-circuit voltage.^{12h}

3. Conclusion

We have developed a novel type of highly efficient starburst organic sensitizers using starburst triarylamine as electron donor moiety, yielding maximum 85% IPCE and 6.02% power conversion efficiency. Introduction of a starburst triarylamine group as the electron-donor unit brought about improved photovoltaic performance comparing with the single triphenylamine unit counterpart. It might be a promising way to inhibit aggregation between molecules and enhance the stability of the solar cells. We present here a new method of bathochromic shifting the absorption spectrum and increasing the molar extinction coefficient of dyes, that is increasing the donor moiety to form D-D- π -A configuration. By adding additional donor moiety to the outside of the donor group, the HOMO and LUMO energy levels can be tuned conveniently. The high oxidation potential and good hole-transporting ability enable them to have the potential of being used as sensitizer and hole-transporting material at the same time, which would simplify the device greatly.

4. Experimental Section

General Procedure for Preparation and Test of Solar Cells. The preparation of dye-sensitized TiO₂ electrode is as follows: 100–150 g·dm⁻³ TiO₂ colloidal dispersion, containing 40 wt% poly(ethylene glycol) (MW-20000), was prepared by following the procedure reported in the literature^{1a} except that autoclaving was performed at 220 °C instead of 200 °C. Optically transparent conducting glass (FTO, transmission >90% in the visible, sheet

resistance 15 Ω /square) was obtained from the Geao Science and Educational Co. Ltd. of China. Films of nanocrystalline TiO₂ colloidal on FTO were prepared by sliding a glass rod over the conductive side of the FTO. Sintering was carried out at 450 °C for 30 min. Before immersion in the dye solution, these films were soaked in the 0.2 M aqueous TiCl₄ solution overnight in a closed chamber, which has been proved to increase the short-circuit photocurrent significantly. The thickness of the TiO₂ film was about 6 μ m. After being washed with deionized water and fully rinsed with ethanol, the films were heated again at 450 °C followed by cooling to 80 °C and dipping into a 3×10^{-4} M solution of dyes in CHCl₃ for 12 h at room temperature. The dye-coated TiO₂ film, as working electrode, was placed on top of an FTO glass as a counter electrode, on which Pt was sputtered. The redox electrolyte was introduced into the interelectrode space by capillary force. The photocurrent action spectra were measured with a Model SR830 DSP Lock-In Amplifier and a Model SR540 Optical Chopper and other optical system. Volt-current characteristics were recorded on Model 2400 Sourcemeter (Keithley Instruments, Inc., U.S.A.) and a 500W xenon lamp was served as a white light source in conjunction with a GRB3 filter. Here a GRB3 neutral filter was used to cut off infrared light to protect the electrode from heating. Masks, which had 0.15 cm² aperture in the middle, were attached on the outside of the glass having dye-adsorbed TiO₂ film. The intensity of the illumination source was measured using a power meter.

Synthesis of (Z)-2-(3-((E)-4-((4-(Diphenylamino)phenyl)(phenyl)amino)styryl)-5,5-dimethylcyclohex-2-enylidene)-2-cyanoacetic acid (S2).²¹ **2** (1 g, 2.27 mmol) and ethyl 2-cyano-2-(3,3,5-trimethylcyclohexylidene)acetate (1.06 g, 4.54 mmol), and piperidine (18 mg, 0.23 mmol) were refluxed in acetonitrile (20 mL) for 8 h under nitrogen atmosphere. After cooling to room temperature, the solvent was removed by vacuum. The resulting coarse product was used in the next step without further purification. The residue ester was hydrolyzed in 2 M LiOH in equal volume of ethanol and water by heating at 50 °C for 5 h. The reaction mixture was diluted by water and the solution pH was adjusted to 6 by adding 1 M HCl at room temperature. The precipitate was then filtered, and purified by silica gel chromatography using ethanol and methylene chloride, and further recrystallization from ethanol solution gave pure S2 as a red powder (yield 55%). ¹H NMR (CDCl₃): δ 7.89 (s, 1H), 7.39 (d, $J = 8.4$ Hz, 2H), 7.32–7.29 (2H), 7.28–7.24 (4H), 7.16 (d, $J = 7.6$ Hz, 2H), 7.10 (d, $J = 8.0$ Hz, 4H), 7.08 (d, $J = 7.6$ Hz, 1H, Ph-H), 7.04–7.01 (8H), 6.99–6.95 (1H), 6.91 (d, $J = 16.0$ Hz, 1H), 2.69 (s, 2H), 2.45 (s, 2H), 1.09 (s, 6H). ¹³C NMR (CDCl₃): 168.1, 167.3, 154.1, 149.2, 147.7, 146.9, 144.0, 141.4, 135.9, 129.5, 129.3, 129.0, 128.6, 128.1, 126.4, 125.0, 125.0, 124.1, 123.8, 123.7, 122.8, 121.5, 117.3, 96.7, 45.1, 39.3, 32.0, 28.2. HRMS: Calcd for C₄₃H₃₈N₃O₂ (M+H)⁺/_z 628.2964. Found: 628.2935.

Synthesis of (Z)-2-(3-((E)-4-(Bis(4-(diphenylamino)phenyl)amino)styryl)-5,5-dimethylcyclohex-2-enylidene)-2-cyanoacetic acid (S3). The synthesis method resembles compound S2 (yield: 58%). ¹H NMR (DMSO): δ 7.79 (s, 1H), 7.52 (d, $J = 8.4$ Hz, 2H), 7.30–7.27 (8H), 7.07–6.91 (22H), 6.88 (d, $J = 8.4$ Hz, 2H), 2.55 (s, 2H), 2.42 (s, 2H), 0.99 (s, 6H). ¹³C NMR (CDCl₃): 165.8, 164.5, 148.7, 147.6, 143.7, 141.6, 135.1, 130.0, 129.4, 129.3, 128.4, 128.0, 126.6, 125.3, 124.5, 124.1, 123.6, 123.3, 120.8, 118.5, 44.5, 38.8, 31.7, 28.2. HRMS: Calcd for C₅₅H₄₇N₄O₂ (M+H)⁺/_z 795.3699. Found: 795.3684.

Synthesis of (Z)-2-(3-((E)-4-(Bis(4-(9H-carbazol-9-yl)phenyl)amino)styryl)-5,5-dimethylcyclohex-2-enylidene)-2-cyanoacetic acid (S4). The synthesis method resembles compound S2 (yield: 67%). ¹H NMR (CDCl₃): δ 8.25 (d, $J = 7.6$ Hz, 4H), 7.85 (s, 1H), 7.73 (d, $J = 9.2$ Hz, 2H), 7.63 (d, $J = 8.8$ Hz, 4H), 7.46–7.43 (12H), 7.31–7.27 (4H), 7.24 (d, $J = 8.8$ Hz, 2H), 7.15 (d, $J =$

(21) Park, K. H.; Twieg, R. J.; Ravikiran, R.; Rhodes, L. F.; Shick, R. A.; Yankelevich, D.; Knoesen, A. *Macromolecules* **2004**, *37*, 5163.

16.0 Hz, 1H), 7.10 (d, $J = 16.4$ Hz, 1H), 2.63 (s, 2H), 0.97 (s, 6H). ^{13}C NMR (CDCl_3): 164.4, 162.7, 147.8, 146.0, 140.7, 134.8, 132.6, 131.5, 129.5, 129.4, 128.4, 128.2, 127.0, 126.6, 126.4, 126.0, 124.0, 123.7, 123.1, 121.0, 120.4, 110.1, 44.5, 38.7, 31.8, 28.2. HRMS: Calcd for $\text{C}_{35}\text{H}_{43}\text{N}_4\text{O}_2$ (M+H)/ z 791.3386. Found: 791.3395.

Synthesis of (Z)-2-(3-((E)-4-(Diphenylamino)styryl)-5,5-dimethylcyclohex-2-enylidene)-2-cyanoacetic acid (S1). The synthesis method resembles compound S2 (yield: 75%). ^1H NMR (CDCl_3): δ 7.89 (s, 1H), 7.36 (d, $J = 7.6$ Hz, 2H), 7.31–7.27 (4H), 7.13 (d, $J = 7.6$ Hz, 4H), 7.08 (d, $J = 7.2$ Hz, 2H), 7.01 (t, $J = 7.6$ Hz, 2H), 6.95 (d, $J = 17.6$ Hz, 1H), 6.91 (d, $J = 16.4$ Hz, 1H), 2.67 (s, 2H), 2.43 (s, 2H), 1.08 (s, 6H). ^{13}C NMR (CDCl_3): 168.9, 167.2, 149.1, 147.0, 135.7, 129.5, 129.4, 128.6, 128.4, 127.7, 125.8, 125.2, 125.1, 123.9, 122.2, 117.2, 45.1, 39.3, 31.6, 28.2. HRMS: Calcd for $\text{C}_{31}\text{H}_{29}\text{N}_2\text{O}_2$ (M+H)/ z 461.2205. Found: 461.2210.

Acknowledgment. This project was partially supported by the NSFC/China (90401026, 50673025), National Basic Research 973 Program (2006CB806200) and Scientific Committee of Shanghai. We are grateful to Dr. Yaoquan Tu and Prof. Hans Ågren in the department of Theoretical Chemistry at the Royal Institute of Technology in Sweden for computational assistance.

Supporting Information Available: ^1H NMR and ^{13}C NMR spectra for the new compounds described in this paper, some optimized geometries and dihedral angle parameters of the compounds, oxidative cyclic voltammetry plot of S4, larger pictures of HOMO–LUMO levels of all compounds. This material is available free of charge via the Internet at <http://pubs.acs.org>.

JO800159T